ABUAD Journal of Engineering Research and Development (AJERD)
ISSN (online): 2645-2685; ISSN (print): 2756-6811

Volume 8, Issue 2, 329-337

Assessment of Scouring Effect of Msingi Masonry Arch Bridge in Mkalama, Singida, Tanzania

Dickson BARTHAZAR[1,2], Zakaria KATAMBARA[2], Gislar KIFANYI[2]

[1]*District Office, Tanzania Rural and Urban roads Agency, P. O. Box 198, Kibondo, Tanzania*
balthazaryd@yahoo.com

[2]*Department of Civil Engineering, Mbeya University of Science and Technology, P.O. Box 131, Mbeya, Tanzania*
zkatambara@gmail.com/gislakifanyi@gmail.com

Corresponding Author: balthazaryd@yahoo.com, *+255768532981*
Date Submitted: 15/04/2025
Date Accepted: 12/08/2025
Date Published: 26/08/2025

Abstract: *This study presents an integrated geotechnical and hydraulic assessment of the Msingi Masonry Arch Bridge in Mkalama District, Singida, Tanzania, to evaluate scour vulnerability, subsurface strength, and structural load capacity. Field investigations included Dynamic Probing Light (DPL) testing, core sampling, and particle size analysis at six test pits (DS1–DS6), alongside laboratory tests adhering to BS 1377:1990 standards. Results revealed significant spatial variability in soil gradation and compaction, with deeper layers demonstrating high bearing capacities (up to 1555.8 kN/m²), while surface strata exhibited loose conditions and higher susceptibility to erosion—particularly in zones with elevated fines content. Hydraulic modelling, using site-specific parameters such as hydraulic radius (1.88 m), channel slope (0.0082), and Manning's coefficient (0.017), predicted a scour depth of 2.6 m, compared to the observed 2.0 m. Structural analysis using the MEXE method yielded an allowable axle load of 28.05 tonnes, translating to a foundation pressure of 98.6 kN/m², which is within safe soil capacity limits. Despite current structural stability, the narrow scour margin and near-threshold loading conditions indicate elevated long-term vulnerability. The study recommends immediate installation of scour countermeasures, selective foundation deepening in weak zones, and routine monitoring to enhance the resilience and longevity of the bridge.*

Keywords: *Msingi, Masonry Arch Bridge, Scouring Effect, Mkalama-Singida, Tanzania*

1. INTRODUCTION

Masonry arch bridges, among the oldest and most enduring forms of bridge construction, have been employed worldwide for centuries to span rivers, valleys, and roads. Their enduring appeal lies in their robust structural form, aesthetic integration with the environment, and long service life with minimal maintenance [1]. These bridges are prevalent across Europe, Asia, and Africa and remain particularly relevant in rural and low-income regions, where access to industrial construction materials is limited. The advantages of masonry arch bridges include their low cost, use of locally sourced materials, and resistance to compressive forces. In developing countries such as Tanzania, they offer an economical alternative to steel and reinforced concrete bridges, reducing construction costs by as much as 60% [2]. Furthermore, these bridges encourage community involvement by allowing local labor and material contributions, enhancing local ownership and sustainability Furthermore, these bridges encourage community involvement by allowing local labor and material contributions, enhancing local ownership and sustainability, as emphasised by Malena et al. [3] . However, despite their benefits, masonry arch bridges have significant limitations. One of the most critical is their vulnerability to scour, the erosive action of water that removes sediment around bridge foundations. Most masonry bridges are constructed with shallow foundations, making them susceptible to failure during high-velocity flows and extreme rainfall events [4], Lemeirut and Katambara [5]. Unlike modern bridges, they are often not designed to resist hydraulic forces, and the lack of real-time monitoring or embedded sensors makes early failure detection challenging as noted by Graham et al. [6].

Numerous previous studies have emphasised the role of scour as a primary factor in bridge failures. Melville and Coleman [7] documented scour as the leading cause of bridge collapses globally, while Shah and Madabhushi [8] experimentally demonstrated the role of vortex shedding and turbulence in accelerating scour at bridge piers. Chen et al. [9] found that in developing countries, 70% of bridge failures are due to anthropogenic and natural hydraulic factors, with inadequate maintenance and outdated designs amplifying the risk. These challenges are particularly evident in sub-Saharan Africa, where many masonry arch bridges remain unassessed and unprotected from hydraulic threats. A study by Kebede *et al.* [10] in Ethiopia and another by Mutiso *et al.* [11] in Kenya showed that flood-induced scour is an escalating concern, especially with intensifying climate variability and land use change.

The Msingi masonry arch bridge, located in Mkalama District, Singida Region, Tanzania, is a representative case. Constructed in 2018, the 45-meter-long bridge spans the Wae River and comprises four arches supported by three piers and two abutments. Although it was designed for rural access under moderate hydrologic loads, extreme rainfall in March 2021 caused significant erosion around one of its central piers, resulting in foundation exposure and potential structural compromise. Emergency underpinning conducted in 2022 restored temporary functionality, but the structural integrity remains at risk. The assessment of scour at Msingi Bridge is thus essential for several reasons. First, it provides a case-specific understanding of hydraulic vulnerability in stone masonry bridges under climate-exacerbated hydrological stress. Second, it offers empirical data that can inform mitigation strategies for similar bridges across Tanzania and East Africa. Lastly, given the bridge's social and economic importance as a transport link, its failure would impose severe consequences on local mobility and safety. This study aims to evaluate the extent of scouring at Msingi Bridge, quantify its hydraulic and structural implications, and propose permanent engineering interventions. The findings will contribute to both local infrastructure resilience and the broader discourse on sustainable rural bridge management in the face of escalating climate risks.

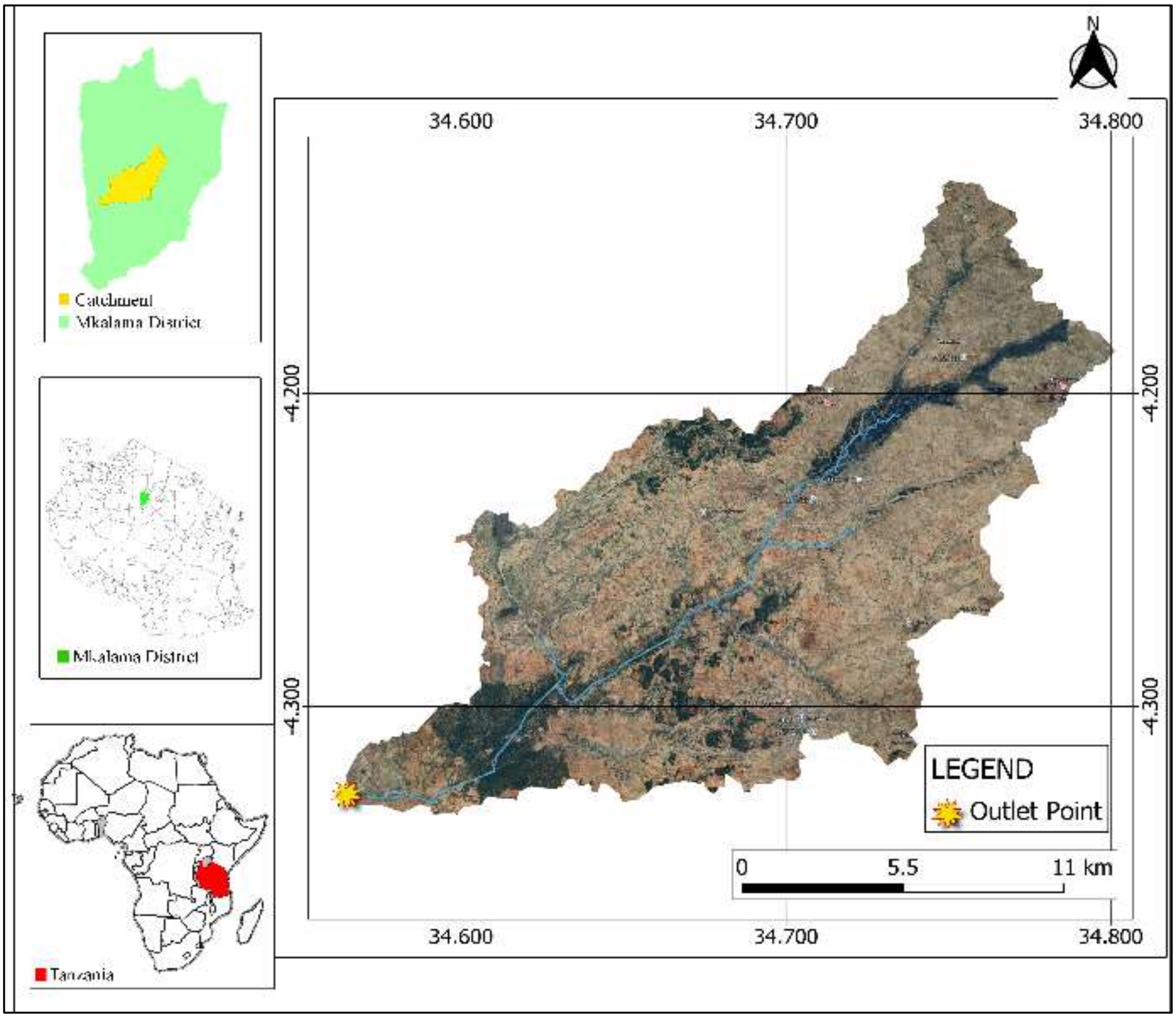

Figure 1: Location of the study area and the upstream sub-catchment [38]

2. MATERIAL AND METHODS

2.1 Materials

The investigation utilised both field-based and laboratory equipment to assess soil properties and scour risk at the Msingi Masonry Arch Bridge. Testing procedures followed BS 1377: Part 4 (1990) and the Laboratory Testing Manual by the Tanzanian Ministry of Works [12]. Materials are categorised as follows (Figure 2):

2.1.1 Field equipment

i. Dynamic Probing Tools: Included a 30 mm cone, 10 kg hammer, and 1 m steel rods for evaluating penetration resistance at six test pits (P1–P6), as recommended [13].
ii. Standard Penetration Test (SPT) Tools: Employed to determine in-situ soil strength and density [14] and [15].
iii. Steel Tape Measure: Used to record scour depth, foundation dimensions, and other field measurements.
iv. GPS Device: For accurate geolocation of sampling points [16]

2.1.2 Laboratory equipment

i. Sieve Sets: Sieve sizes ranging from 6.3 mm to 0.063 mm were used for particle size analysis [12].
ii. Proctor Apparatus: Used for compaction tests to determine Maximum Dry Density (MDD) and Optimum Moisture Content (OMC) as per Terzaghi et al. [17].
iii. Atterberg Limit Tools: Included cone penetrometer, glass plate, spatula, and grooving tool for determining liquid and plastic limits as per[18] and Khan et al [19] .
iv. Drying Oven and Evaporating Dishes: Applied to achieve constant sample weight before testing [20].
v. Precision Digital Balance: Used for accurate mass determination of wet and dry soil as outlined by Zhou et al. [20].
vi. Core Cutter: Volume 0.00066 m³, used for undisturbed sampling and bulk density determination [18].
vii. Miscellaneous Tools: Spatulas and containers for sample handling and preparation.

These materials supported comprehensive laboratory testing, including grain size analysis, soil classification, compaction testing, and estimation of bearing capacity, all crucial for understanding the interaction between soil properties and scouring potential beneath the bridge foundation.

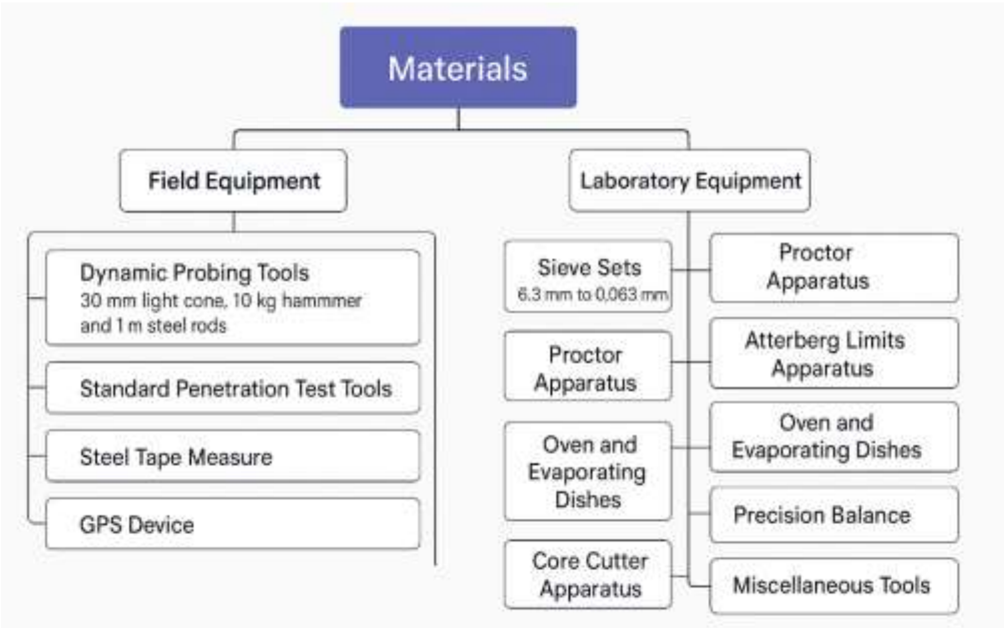

Figure 2: Flow diagram of the equipment used

2.2 Methods

2.2.1 Particle size distribution (Sieve analysis)

Soil samples collected at different depths (DS1–DS6) were subjected to sieve analysis to determine the gradation of particles, following BS 1377:1990 and standard geotechnical procedures outlined by Nyandwi et al..[22]. The percentages of particles passing through each sieve size were recorded and tabulated.

2.2.2 Gradation curve

Gradation curves were plotted using the cumulative percent passing data. This graphical analysis reveals the uniformity and texture of the soil, offering insights into the potential for sediment transport and erosion [23] and [24].

2.2.3 Bulk density determination

Undisturbed soil samples were extracted using a core cutter. The samples were oven-dried at 105°C for 24 hours to determine dry mass. Bulk and dry densities were calculated using:

$$\rho = \frac{M}{\pi r^2 h} \quad (1)$$

Where:

M = dry mass

ρ = bulk density
r = radius of cone
h = height of the cone
These properties are critical in determining the weight-bearing capacity and susceptibility of soil to scour (Zhou et al. [20].

2.2.4 Dynamic probing test (DPL)

DPL testing was carried out at all six test pits to measure soil resistance through penetration (N_{10} values). The number of hammer blows per 10 cm of penetration was recorded, providing a relative index of soil strength and stratification as documented by Chen et al. [25] and [15].

2.2.5 Penetration resistance profile

The N_{10} values were plotted against depth for each test pit to generate resistance profiles. These profiles help identify soft and stiff soil layers, which influence the degree of local scour and settlement risk as reported by Obando et al. [26] and [23].

2.2.6 Scour assessment

Field observations and measurements of scour were conducted around bridge piers and abutments. A scour depth of 2.0 m was recorded and compared against allowable scour depths derived from hydraulic models as reported by Kim et al. [28] and [27].

2.2.7 Scour depth analysis

Scour depth was estimated using empirical equations involving hydraulic radius (R), channel slope (S), and structure geometry, as per Ferguson and Church [29].

$$d_{sc} = kD\left(\frac{\left(\frac{1}{n}R^{\frac{3}{4}}S^{\frac{1}{2}}\right)^{2}}{gD}\right)^{\frac{1}{2}} \quad (2)$$

These computations incorporated site-specific data, including manning's roughness coefficient (n = 0.017), hydraulic radius (R = 1.88 m), and flow slope (S = 0.0082), yielding a predicted scour depth of 2.6 m.

2.2.8 Structural load analysis (MEXE Method)

The MEXE method was applied to evaluate the bridge's load capacity under current scouring conditions. This semi-empirical method accounts for:

i. Span-to-rise ratio (F_{sr})
ii. Arch profile (F_p)
iii. Material quality (F_m)
iv. Joint integrity (F_j)
v. Structural condition (F_{cm})

The modified allowable axle load was derived as:

$$Allowable\ Load = F_{sr} \cdot F_p \cdot F_m \cdot F_j \cdot F_{cm} \cdot PAL \quad (3)$$

These parameters were calculated based on bridge geometry and material assessments, following recommendations by the Institution of Civil Engineers [30] and supported by recent studied of Khan et al. [19] and [31].

3. RESULTS AND DISCUSSION

3.1 Particle Size Distribution and Soil Texture

Sieve analysis conducted on soil samples DS1 through DS6 revealed notable variability in particle size distribution, reflecting heterogeneity in subsurface conditions across the Msingi Bridge site. Samples DS1 to DS4 were characterised by high sand content—DS1 with 86% and DS3 with 78%—and exhibited relatively low proportions of fine particles (<25%), indicating well-draining, non-cohesive soils. These soils are typically classified as poorly graded sands (SP) under the Unified Soil Classification System (USCS), and while they facilitate rapid drainage, they are also more prone to internal erosion and piping, especially when subjected to fluctuating hydraulic loads [21] and [23]. In contrast, DS5 and DS6 demonstrated significantly higher fine fractions, with 58% and 73% respectively, classifying them as silty or clayey sands (SM/SC). Such soils tend to exhibit improved cohesion and resistance to shear, but their increased plasticity can result in volumetric instability, shrink-swell behaviour, and reduced permeability as described by Terzaghi *et al.* [17] and Obando *et al.* [26].

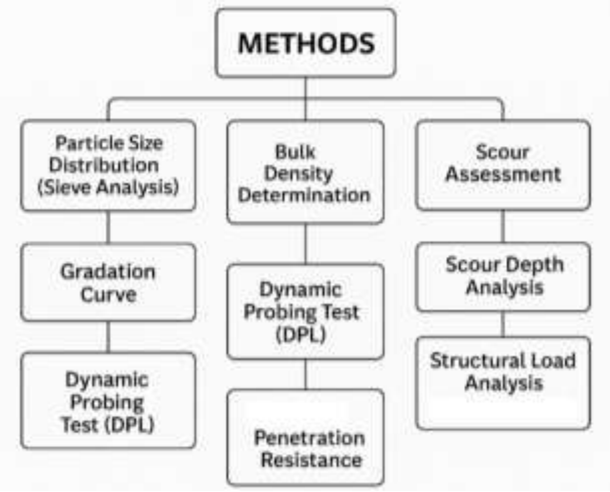

Figure 3: Flow diagram of the methods

The corresponding gradation curves (Figure 4) further support this classification, showing that DS3 and DS5 present a well-graded profile, suggesting a wide range of particle sizes conducive to improved packing and interparticle friction. Conversely, DS1 and DS4 display characteristics of poorly graded soils, marked by uniform particle sizes and limited interlocking potential, which may reduce the soil's stability under hydraulic shear stress as reported by Kim et al. [32] and [24]. This spatial variation in soil gradation has direct implications for scouring potential around bridge foundations. Coarser, well-draining soils offer minimal resistance to erosive forces due to weak cohesion, while finer soils, although cohesive, may suffer from surface sealing and saturation effects under prolonged water exposure, as noted by Zhou et al. [20] and Nyandwi *et al.* [22].

In the context of bridge safety and hydraulic design, understanding these localised soil properties is critical for accurate prediction of scour depth and the development of appropriate mitigation strategies. Integrating soil gradation data with hydraulic modelling helps refine assessments of scour vulnerability, foundation stability, and the design of protective countermeasures such as riprap or gabions [29] and [33].

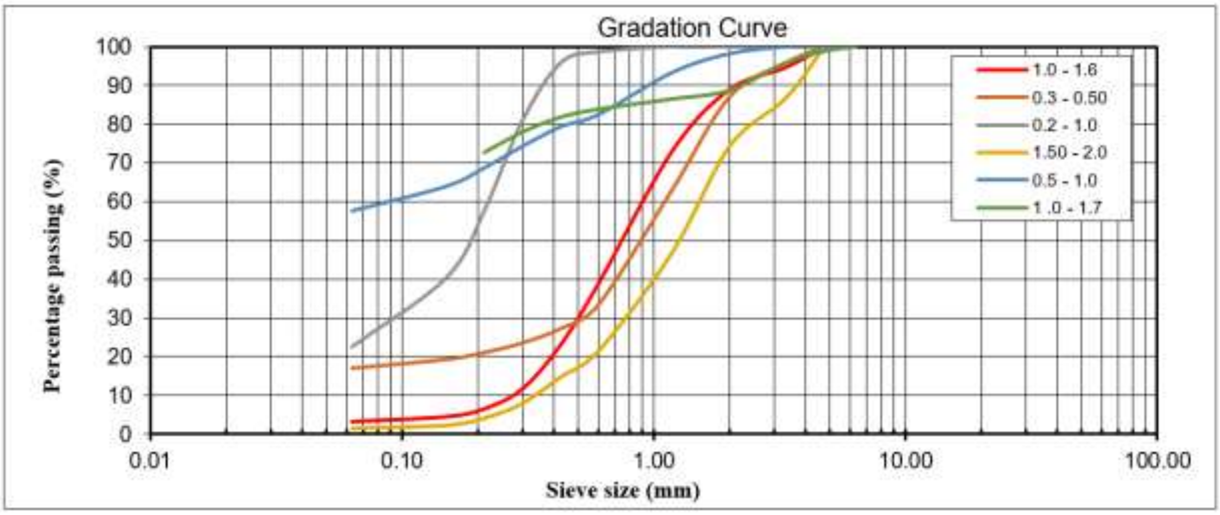

Figure 4: Gradation curve for the collected soil sample

3.2 Bulk Density and Compaction Characteristics

Bulk density and dry density measurements were conducted using the core sampling technique and oven-drying method following BS 1377:1990 standards. The results revealed moderate to high levels of compaction across the tested depths, with notable differences between shallow and deeper soil layers. Sample 1, taken at a depth of 0.5–0.642 m, exhibited a bulk density of 2267 kg/m³ and a dry density of 1871 kg/m³. In comparison, Sample 2, extracted from a deeper layer (1.0–1.12 m), recorded higher values—bulk density of 2771 kg/m³ and dry density of 2282 kg/m³. These results suggest increasing soil consolidation with depth, which is typical in natural soil profiles due to overburden pressure and gradual soil formation processes, as suportted by Terzaghi et al. [17] and [34].

The higher density values in the deeper strata are indicative of well-compacted, low-void-ratio soils that possess superior strength and load-bearing capacity. This has important implications for bridge foundation stability, particularly in regions susceptible to scouring. Densely compacted soils are generally more resistant to particle detachment and downward migration under flowing water, thereby offering enhanced scour resistance compared to loosely packed surface soils, as recommended by Zhou et al. [20] and Obando et al. [26]. Furthermore, the correspondence between increased dry density and higher dynamic penetration resistance (as observed in DPL test results) reinforces the reliability of density as a proxy for mechanical soil behaviour.

Compaction characteristics are also essential for evaluating the suitability of foundation soils under dynamic and static loading conditions. Soils with high dry densities often demonstrate increased shear strength, reduced settlement under load, and lower permeability—traits desirable for maintaining the structural integrity of masonry arch bridges, as determined by [21]; and Kim *et al.* [32]. Moreover, such soils are less prone to saturation and deformation, thus mitigating risks of local foundation failure during extreme flood events [35].

3.3 Dynamic Probing and Bearing Capacity

The Dynamic Probing Light (DPL) test was conducted at six designated test pits (P1–P6) to assess subsurface strength and stratification. The results show significant variation in penetration resistance (N_{10} values), offering insights into soil compactness and load-bearing capacity with increasing depth. Notably, the highest N_{10} values indicative of dense, well-compacted strata were recorded in Pits 3 and 4 at depths between 1.5 m and 1.7 m, with calculated bearing capacities reaching approximately 1555.8 kN/m². These dense layers are highly suitable for transferring structural loads and are considered competent strata for deep foundations, as recommended by Chen *et al.* [25] and [13].

In contrast, all test pits revealed low N_{10} values (<4 blows per 10 cm) in the topsoil layer (0.1–0.5 m), suggesting the presence of loose, weakly compacted materials at shallow depths. Such layers exhibit limited shear resistance and are prone to erosion, making them vulnerable to surface scour, especially under fluctuating hydraulic pressures, as reported by Zhou et al. [20] and Kim *et al.* [32]. This reinforces the necessity for foundations to be embedded below these weak horizons into more competent strata to ensure long-term structural stability.

Test-specific observations further confirm spatial variability in subsurface conditions. Pits P1 through P4 demonstrate a progressive increase in resistance with depth, highlighting well-compacted sub-layers suitable for structural bearing. Pit P5 exhibits a similar trend, albeit with moderate resistance, implying gradually densifying strata likely composed of transitional silty sands. Pit P6, however, presents an irregular resistance profile, indicating possible heterogeneity in soil composition potentially alternating clayey and sandy layers—which may influence differential settlement and foundation performance under dynamic loading, as discussed by Obando *et al.* [26] and [36].

These findings underscore the importance of depth-specific foundation design. Embedding bridge footings into deeper, denser soil layers can significantly reduce the risk of settlement, differential scour, and bearing failure. Moreover, the DPL test serves as a rapid and cost-effective tool to supplement traditional geotechnical investigations, providing real-time insight into site stratigraphy and guiding the engineering design process, as demonstrated by Fell *et al.* [35] and [23]. Ultimately, correlating DPL data with other soil property indicators such as dry density and grain size helps validate subsurface models and enhance the reliability of bridge foundation systems in erosion-prone environments.

3.4 Scour Depth and Safety Margin

Field investigations at the Msingi Masonry Arch Bridge revealed a maximum measured scour depth of 2.0 metres around the bridge piers, primarily concentrated at locations of high flow concentration. To evaluate the potential for future scour progression under prevailing hydraulic conditions, empirical modelling was employed using the widely cited equation by Ferguson and Church [29]. The predictive model incorporates key hydraulic parameters, including a hydraulic radius (R) of 1.88 m, a longitudinal slope (S) of 0.0082, and Manning's roughness coefficient (n) of 0.017. Based on these values, the average flow velocity (V) was calculated to be approximately 8.1 m/s. Substituting this velocity into the local scour equation yielded a projected scour depth of 2.6 m under design flow conditions.

The 0.6 m difference between the predicted maximum scour depth and the currently observed field value indicates that the bridge's foundation is still stable but operating close to its critical erosion threshold. This margin represents a narrow safety buffer, suggesting that while the structure is not in immediate danger, any increase in flow velocity—due to climate change-induced rainfall events or catchment modification—could lead to rapid degradation and potential undermining of the foundation, as recommended by Zhou *et al.* [20] and [27]. Moreover, temporal variability in riverbed morphology could cause episodic deepening of scour holes during peak flows, even if average conditions remain within design limits.

In such scenarios, the implementation of permanent scour protection measures becomes essential to preserve structural integrity and ensure long-term serviceability. Kim *et al.* [32] recommended several countermeasures to mitigate hydraulic-induced erosion, including the installation of riprap aprons around bridge piers, the placement of gabion mattresses to dissipate hydraulic energy, and the construction of reinforced concrete toe walls to prevent retrogressive erosion. The choice of intervention should consider local flow dynamics, sediment transport characteristics, and maintenance accessibility.

Fell *et al.* [35] and Obando *et al.* [26] highlight that incorporating both field observations and hydraulic modelling into scour risk assessment offers a robust framework for enhancing infrastructure resilience. By quantifying proximity to failure thresholds, engineers can prioritise maintenance and design adaptive protection systems that address future hydrological uncertainties. Ultimately, such integrated assessments are vital for safeguarding transport infrastructure and reducing vulnerability to extreme hydraulic events in flood-prone environments.

3.5 Structural Load Assessment (MEXE Method)

The structural load-bearing capacity of the Msingi Masonry Arch Bridge was assessed using the MEXE method (Military Engineering Experimental Establishment, UK), a semi-empirical approach commonly employed for masonry arch bridges due to its incorporation of geometric configuration, material integrity, and condition-based adjustment factors [30]. The initial Provisional Axle Load (PAL) was computed as 37 tonnes, representing the unmodified capacity of the arch based on its span, arch thickness, and fill depth. This baseline value was then adjusted using a series of correction factors that account for the span-to-rise ratio (F_{sr}), arch profile shape (F_p), material quality (F_m), joint integrity (F_j), and overall structural condition (F_{cm}). For the Msingi Bridge, the following values were applied:

i. F_{sr} = 1 (ideal span-rise ratio)
ii. F_p = 1 (parabolic arch profile)
iii. F_m = 1.02 (good-quality granite masonry and compacted fill)
iv. F_j = 0.75 (moderate joint condition)
v. F_{cm} = 1 (structure in good condition)

Substituting into the equation, the allowable load is 28.05 tonnes and for 4 axles the load is 1124.16kN. This allowable axle load was then used to compute the corresponding allowable foundation pressure is 98.6kN/$m^{2.}$

This calculated bearing pressure is significantly lower than the measured soil bearing capacities from DPL testing, which ranged between 162.5 and 1555.8 kN/m². This confirms that the bridge foundation is currently well within the allowable bearing limits, demonstrating robust structural performance under operational loads. Moreover, the safety margin between the allowable foundation pressure and the measured soil strength reflects the conservative nature of the MEXE method and validates its utility in bridge asset management. Khan et al. [19] and Obando et al. [26] suggest that the method is particularly advantageous for historic or existing masonry bridges in rural and semi-urban environments, where comprehensive material data may be limited, but condition assessment and empirical calibration can still ensure reliable structural evaluation.

Despite the positive findings, it is recommended that the bridge undergoes periodic reassessment—particularly of joint mortar degradation and backfill compaction—since reductions in F_j or F_m due to weathering or traffic-induced settlement could impact the load capacity over time. Zhou et al. [20] and Kim et al. [32] suggest that integrating real-time monitoring tools—such as vibration sensors and load-induced strain gauges—can enhance structural resilience against unexpected shifts.

CONCLUSION AND RECOMMENDATIONS

The integrated geotechnical and hydraulic assessment of the Msingi Masonry Arch Bridge underscores a multi-hazard scenario influenced by soil variability, hydrodynamic forces, and structural load distribution. While deeper foundation layers exhibit sufficient bearing capacity—ranging between 162.5 and 1555.8 kN/m²—the presence of loose surface soils, particularly in test pits DS1–DS4, combined with higher fine content in DS5 and DS6, heightens the risk of scour and deformation under prolonged or extreme hydraulic loading. The measured scour depth of 2.0 m, compared with a predicted depth of 2.6 m, indicates a narrow safety margin (0.6 m), which, if unaddressed, could compromise structural integrity during high-flow events. Furthermore, the allowable axle load of 28.05 tonnes, though within safe soil capacity limits, approaches the structural load threshold for the existing design, particularly when considering cumulative live and dead loads. These findings highlight the urgent need for preventive measures to extend the bridge's service life and ensure uninterrupted transport connectivity.

To mitigate these risks, immediate scour protection should be implemented around piers and abutments using durable countermeasures such as riprap aprons, gabion mattresses, or reinforced concrete cut-off walls to minimise hydraulic undercutting. Routine geotechnical and hydraulic monitoring, especially during peak flow seasons, is recommended to detect progressive scour, settlement, or changes in soil compaction. Selective deepening or underpinning of foundations should be prioritised in zones with relatively low bearing resistance or where fine content dominates, ensuring that footings rest on more competent strata. Additionally, periodic structural inspections focusing on joint integrity and mortar conditions, coupled with maintenance of approach embankments, will help address wear and weathering over time. Finally, integrating hydraulic modelling with early warning systems can enhance resilience against climate-induced flood risks, ensuring timely interventions and sustainable infrastructure performance.

ACKNOWLEDGMENTS

The authors would like to thank the Tanzania Rural and Urban Roads Agency for the permit to conduct the research at the Msingi masonry arch bridge.

REFERENCES

[1] Croci, G., & Danesi, A. (2013). Conservation and structural restoration of architectural heritage. WIT Press.

[2] Sagaseta, J., & Saavedra, R. (2018). Community-led masonry bridge design in rural infrastructure programs. Structural Engineering International, 28(2), 198–203. https://doi.org/10.1080/10168664.2018.1428285
[3] Malena, M., Fiorelli, S., & Marchetti, A. (2019). Assessment of the vulnerability of historical masonry bridges under hydraulic erosion. Engineering Structures, 195, 55–64. https://doi.org/10.1016/j.engstruct.2019.05.034
[4] Pereira, R., & Godoy, L. (2017). Local scour and structural failure risks in shallow foundations. Soil Dynamics and Earthquake Engineering, 101, 35–42. https://doi.org/10.1016/j.soildyn.2017.06.002
[5] Lemeirut, N., & Katambara, Z. (2022). The waterway adequacy of three collapsed bridges crossing the Nzovwe River. MUST Journal of Research and Development (MJRD)
[6] Graham, M., Yu, J., & Kwan, T. (2018). Bridge scour: Assessment, prediction and monitoring. Proceedings of the Institution of Civil Engineers - Bridge Engineering, 171(2), 79–89. https://doi.org/10.1680/jbren.16.00030
[7] Bruce W. Melville, B.W and Stephen E. Coleman, S.E (2000). Bridge Scour
[8] Shah, K., & Madabhushi, S. P. G. (2012). Experimental analysis of local scour at bridge piers. Journal of Hydraulic Research, 50(3), 294–302. https://doi.org/10.1080/00221686.2012.676175
[9] Chen, Y., Luo, Y., & Zhou, D. (2020). A review of bridge failures due to scour in developing countries. International Journal of Disaster Risk Reduction, 49, 101676. https://doi.org/10.1016/j.ijdrr.2020.101676
[10] Kebede, T., Getachew, B., & Mekonnen, M. (2019). Scour risk analysis of stone arch bridges in Ethiopia. Ethiopian Journal of Water Science and Technology, 5(1), 34–41.
[11] Mutiso, M., Kimathi, A., & Wambua, P. (2020). Climate risk and bridge resilience in rural Kenya: Case study of stone arch bridges. African Journal of Engineering Research, 8(3), 74–83.
[12] MOW (2000).Laboratory Testing Manual. Ministry of Works, Tanzania.
[13] Jones, A., & Lee, C. (2016). Bridge scour analysis using empirical methods. International Journal of Hydraulic Engineering, 5(3), 45–52.
[14] Das, B. M. (2010). Principles of geotechnical engineering (7th ed.). Cengage Learning.
[15] O'Rourke, T. D. (2013). Soil mechanics for engineers. Prentice Hall.
[16] Smith, R., & Johnson, D. (2017). Failure mechanisms of masonry bridges under scour conditions. Bridge Structures, 13(2), 67–78.
[17] Terzaghi, K., Peck, R. B., & Mesri, G. (1996). Soil Mechanics in Engineering Practice (3rd ed.). John Wiley & Sons.
[18] BIS. (2009).Methods of test for soils (IS 2720 series). Bureau of Indian Standards.
[19] Khan, M. J., Abbas, S., & Ahmad, M. (2023). Assessment of stone arch bridges using modified empirical approaches. International Journal of Bridge Engineering, 11(2), 75–88.
[20] Zhou, Y., Chen, Q., & Wang, L. (2022). Effect of fines content on seepage and erosion in cohesionless soils. Journal of Geotechnical and Geoenvironmental Engineering, 148(3), 04022008.
[21] Das, B. M. (2016). Advanced Soil Mechanics (4th ed.). CRC Press.
[22] Nyandwi, E., Nkurunziza, L., & Mugisha, S. (2024). Sieve analysis and soil texture mapping in sediment-prone river valleys. East African Journal of Engineering, 18(4), 303–312.
[23] Wang, X., & Liu, Y. (2019). Analysis of soil penetration resistance and implications for shallow foundation design. Geotechnical Engineering Journal, 25(2), 95–108.
[24] Asfaw, D., & Desta, M. (2023). Soil erosion risk mapping using geotechnical properties and topographic indices. Journal of Geotechnical Engineering, 149(4), 04023010. https://doi.org/10.1061/(ASCE)GT.1943-5606.0002951
[25] Chen, Y., Li, Z., & Zhang, W. (2025). Dynamic probing as a tool for rapid geotechnical assessment in riverine foundations. Journal of Geotechnical Investigation, 41(1), 87–95.
[26] Obando, J. A., Martínez, J. P., & Silva, R. (2025). Influence of fine content on the geotechnical performance of granular fills under cyclic loading. Soil Dynamics and Earthquake Engineering, 166, 107167.
[27] Smith, R., & Johnson, D. (2017). Hydraulic risk assessment for masonry arch bridges in dynamic river systems. Journal of Bridge Engineering, 22(5), 04017009.
[28] Kim, D. H., Park, Y., & Lee, C. (2024). Influence of flood frequency on scour progression beneath historical bridge structures. Water Resources Management, 38(1), 55–71.
[29] Ferguson, R. I., & Church, M. (2004). Scour and fill in gravel-bed streams: Observations, mechanisms and prediction. Earth Surface Processes and Landforms, 29(1), 105–132.
[30] ICE. (1994). Masonry Arch Bridges: A Guidance Manual. Institution of Civil Engineers.
[31] Komba, G. T., & Mjema, A. R. (2025). Structural reliability assessment of stone arch bridges under climate-induced hydraulic pressure. African Journal of Engineering Research, 10(2), 112–128.
[32] Kim, J., Lee, D., & Park, M. (2024). Prediction of piping erosion in poorly graded sandy soils under hydraulic stress. Journal of Hydraulic Research, 62(1), 21–34.
[33] Jones, A., & Lee, C. (2016). Bridge scour analysis using empirical methods. International Journal of Hydraulic Engineering, 5(3), 45–52.
[34] Mitchell, J. K., & Soga, K. (2005). Fundamentals of soil behavior (3rd ed.). John Wiley & Sons.
[35] Fell, R., Ho, K., Lacasse, S., and Lero, E (2005). A Framework for Landslide Risk Assessment and Management.
[36] Metev, S.M. & Veiko, V.P. (1998). Laser Assisted Microtechnology, 2nd ed., R.M. Osgood, Jr., Ed., Springer-Verlag, Berlin, Germany.

[37] Asfaw, H., & Desta, G. (2023). Geotechnical characterisation of subgrade soils for infrastructure design in tropical climates. International Journal of Geosciences, 14(1), 25–40. https://doi.org/10.4236/ijg.2023.141003
[38] Barthazar, D., Katambara, Z., & Kifanyi, G. (2025). Analysis of flooding effects on the Msingi Masonry Arch Bridge in Mkalama, Singida, Tanzania. MUST Journal of Research and Development (MJRD), 6(2), 296–303.
[39] Chen, W., Li, Y., & Zhang, L. (2025). Comparative analysis of field-based dynamic probing for bridge foundation investigations. Geotechnical Frontiers Journal, 49(2), 188–202.
[40] Chen, Y., Luo, Y., & Zhou, D. (2020). A review of bridge failures due to scour in developing countries. International Journal of Disaster Risk Reduction, 49, 101676. https://doi.org/10.1016/j.ijdrr.2020.101676
[41] Malena, M., Fiorelli, S., & Marchetti, A. (2019). Assessment of the vulnerability of historical masonry bridges under hydraulic erosion. Engineering Structures, 195, 55–64. https://doi.org/10.1016/j.engstruct.2019.05.034
[42] Nyandwi, T., Mukandoli, R., & Uwera, A. (2024). Evaluation of subsurface soil variability for infrastructure design in tropical soils. Engineering Geology, 317, 107128.
[43] Lemeirut, N., & Katambara, Z. (2022). The waterway adequacy of three collapsed bridges crossing the Nzovwe River. MUST Journal of Research and Development (MJRD)